

---

# Validation of Nitrogen-13-Ammonia Tracer Kinetic Model for Quantification of Myocardial Blood Flow Using PET

Otto Muzik, Rob S.B. Beanlands, Gary D. Hutchins, Tom J. Mangner, Ngoc Nguyen and Markus Schwaiger

*Division of Nuclear Medicine, Department of Internal Medicine, University of Michigan Hospitals, Ann Arbor, Michigan*

---

Positron emission tomography has been shown to provide quantitative estimates of myocardial blood flow using  $^{13}\text{N}$ -ammonia and  $^{15}\text{O}$ -water. In a validation study, myocardial blood flow was noninvasively determined in 11 open-chest anesthetized dogs using dynamic positron emission tomography. The radiopharmaceuticals  $^{13}\text{N}$ -ammonia and  $^{15}\text{O}$ -water were intravenously administered and measurements were carried out at rest and following pharmacological vasodilation to assess blood flow over a range from 53 to 580 ml/100 g/min. Quantification of blood flow based on tracer kinetic modeling of  $^{13}\text{N}$ -ammonia data correlated closely with myocardial blood flow determined by microspheres ( $y = 0.944 \times +7.22$ ,  $r = 0.986$ ) and with the  $^{15}\text{O}$ -water injection technique ( $y = 1.054 \times -15.8$  ( $r = 0.99$ )). The use of  $^{13}\text{N}$ -ammonia with positron emission tomography enables the accurate quantification of myocardial blood flow. Using this technique, uncomplicated study protocols simplify the measurement procedures while providing excellent qualitative and quantitative information.

**J Nucl Med 1993; 34:83-91**

---

**A**bsolute quantification of regional myocardial blood flow allows the determination of coronary flow reserve; a parameter proposed for the measurement of the functional integrity of the coronary vasculature (1). Several invasive methods have been applied to determine this parameter, including coronary angiography (2), doppler flow probe and the thermodilution technique (3). The clinical demand for such measurements has led to the investigation of noninvasive approaches using positron emission tomography to quantify flow and flow reserve. The dual photon emission process from positron-electron annihilation allows accurate attenuation correction and enables the absolute quantification of the temporal behavior of tissue radionuclide concentrations in the human organism.

---

Received Mar. 24, 1992; revision accepted Jul. 31, 1992.  
For reprints or correspondence contact: Markus Schwaiger, MD, Professor of Internal Medicine, Division of Nuclear Medicine, Department of Internal Medicine, University of Michigan Hospitals, 1500 E. Medical Center Dr., B1G412, Ann Arbor, MI 48109-0028.

Standard tracer kinetic methods can then be employed to estimate the rates of physiologic processes in various organs including flow.

The positron emission tomography (PET) radiotracers which have shown the most promise for quantification of myocardial blood flow are  $^{15}\text{O}$ -water and  $^{13}\text{N}$ -ammonia. Oxygen-15-water is assumed to behave as an inert freely diffusible tracer. Therefore, the Kety-Schmidt techniques for the analysis of blood flow using inert tracers can be applied. Successful applications of this technique have been presented by several investigators (4,5). The primary limitations of the  $^{15}\text{O}$ -water perfusion method result from the limited count rate capabilities of most available tomographic systems and the poor tissue to blood contrast ratios achieved throughout the study making the delineation of myocardial tissue difficult. Therefore, an additional  $\text{C}^{15}\text{O}$  scan is necessary for each blood flow measurement in order to position myocardial regions of interest and to perform the blood volume correction. At the present time, the combination of tomograph performance and study complexity limit the widespread clinical application of this approach (4).

The application of radiotracers which behave similar to radiolabeled microspheres represents an alternative approach for the measurement of myocardial perfusion. One such tracer is  $^{13}\text{N}$ -ammonia, which is avidly extracted by the myocardium and retained with a long biological half-life (6).

The advantages of  $^{13}\text{N}$ -ammonia as a myocardial perfusion tracer include acceptable tomograph count rates and high tissue to blood contrast ratios enabling clear delineation of the walls of the myocardium. The use of  $^{13}\text{N}$ -ammonia for quantification of myocardial blood flow has been compromised by the nonlinear relationship between tracer tissue retention and myocardial blood flow (7). The initial extraction of this tracer, however, has been shown to be largely independent of blood flow (6). Recently, a tracer kinetic model has been developed enabling the separation of initial extraction of  $^{13}\text{N}$ -ammonia into extravascular space from myocardial retention through metabolic conversion to glutamine. The application of this model enables the quantification of myocardial blood flow over a wide flow range (8).

The purpose of this study was to validate the three-compartment kinetic model for myocardial blood flow measurements using  $^{13}\text{N}$ -ammonia developed at our institution. Blood flow estimates with  $^{13}\text{N}$ -ammonia were compared to those obtained with  $^{15}\text{O}$ -water in the dog model. Both PET flow measurements were correlated with microsphere determined blood flows over a wide flow range.

## MATERIALS AND METHODS

The study protocol (Figure 1) was approved by the Committee for Animal Research at the University of Michigan, and performed in accordance with the "Position of the American Heart Association on Research Animal Use" (9).

### Experimental Preparation

Eleven mongrel dogs weighing 15–20 kg (mean 18.2 kg) were anesthetized with intravenous pentobarbital (30 mg/kg). All dogs were intubated and ventilated with oxygen-enriched room air (Harvard Apparatus). A peripheral venous line was placed for drug injection and a femoral venous line for administration of isotopes. Cannulae were inserted into the abdominal aorta via the femoral artery bilaterally for systemic pressure monitoring and for arterial blood sampling. The ECG was monitored continuously. A left thoracotomy was performed and the heart carefully suspended in a pericardial cradle. A left atrial catheter was inserted via the left atrial appendage for microsphere injection. The left atrial position of this catheter was confirmed by a left atrial pressure tracing. The left circumflex artery was isolated and a doppler flow probe gently placed around it to monitor online coronary flow during different experimental states. The pericardial cradle was then released, all catheters and wires exteriorized to the abdomen and the chest closed. All hemodynamic measurements and ECG were recorded on a multichannel strip chart recorder (Hewlett Packard 7848A).

### PET Data Acquisition

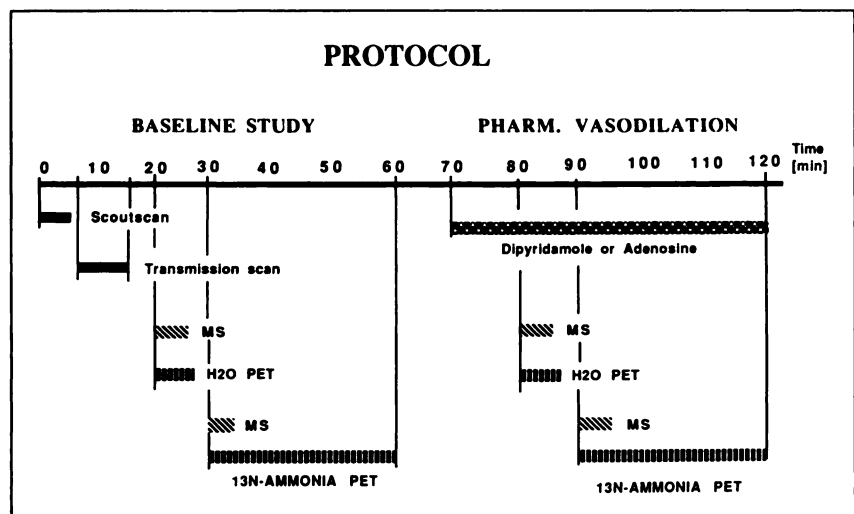
Each dog was then positioned in the positron emission tomograph (PCT4600A, TCC Corp) (10). This scanner consists of three rings of 96 bismuth germanate crystals with a center-to-

center separation of 23 mm that are able to acquire coincidence data in three direct planes and two cross-planes normalized to the direct planes. The data is reconstructed using a Hanning filter into five transverse image planes of 1.1 cm thickness with an in-plane resolution of 12.5 mm FWHM. An intravenous bolus of 0.5 mCi of  $^{13}\text{N}$ -ammonia was used to perform a scout scan of the thorax to align the heart with the field of view of the scanner. A 10 min transmission scan using a  $^{18}\text{F}$  ring source was then acquired and subsequently used to generate attenuation correction factors.

**Baseline Studies.** Following stabilization of hemodynamic parameters, 3–5 mCi of  $^{15}\text{O}$ -water diluted in 10 cc of normal saline was injected via the femoral vein (over 10 sec in 5 dogs and over 25 sec in the remainder), and radiolabeled microspheres were injected into the left atrium. The arterial input function for  $^{15}\text{O}$ -water was determined by withdrawal of 1 ml serial samples of arterial blood ( $20 \times 6 \text{ sec}/12 \times 15 \text{ sec}$ ). Activity was immediately counted in a well counter (EG & G Ortec), and automatically corrected for background and decay. For the microsphere studies, the arterial input function was determined by withdrawal of arterial blood from the abdominal aorta at a constant rate of 14.16 ml/min using a Harvard pump (Gould, Inc.) At the time of the  $^{15}\text{O}$ -water injection, simultaneous dynamic image acquisition was initiated with varying frame duration ( $12 \times 5 \text{ sec}/16 \times 15 \text{ sec}$ ). The total scanning time was 5 min. After acquisition of the baseline  $^{15}\text{O}$ -water study, at least 10 min were allowed for decay of  $^{15}\text{O}$  (physical half-life 123 sec).

For the  $^{13}\text{N}$ -ammonia flow studies, 3 to 5 mCi of  $^{13}\text{N}$ -ammonia diluted in 10 cc of normal saline was injected via the femoral vein. One ml blood samples were withdrawn from an arterial line ( $20 \times 6 \text{ sec}/10 \times 30 \text{ sec}/2 \times 90 \text{ sec}$ ). One milliliter samples were also drawn at 1, 3, 5 and 10 min after injection for assessment of  $^{13}\text{N}$ -ammonia metabolites. Radiolabeled microspheres were injected into the left atrium and the arterial input function was determined by withdrawal of arterial blood as described above. As with  $^{15}\text{O}$ -water, a simultaneous dynamic image acquisition was initiated at the time of the  $^{13}\text{N}$ -ammonia injection with varying frame duration ( $12 \times 10 \text{ sec}/4 \times 30 \text{ sec}/3 \times 120 \text{ sec}$ ). In five studies, four 300 sec scans were added at the end for a total acquisition time of 30 min. After acquisition of the baseline  $^{13}\text{N}$ -ammonia study, at least 50 min was allowed for decay of  $^{13}\text{N}$

**FIGURE 1.** Protocol used to acquire data from PET scans using the agents  $^{13}\text{N}$ -ammonia and  $^{15}\text{O}$ -water. Radiolabeled microspheres (MS) were administered concomitantly with each dynamic scan sequence. After the acquisition of the baseline study was completed, blood flow was increased through pharmacological intervention and both dynamic scans repeated.



(physical half-life 9.9 min). During this time, residual  $^{13}\text{N}$  activity from the preceding experiment had physically decayed to <3% of its initial activity.

**Pharmacological Interventions.** The study protocol was the same as described above for the baseline studies. Myocardial blood flow was increased by intravenous adenosine infusion of 0.14–0.5 mg/kg/min in three dogs. Because of difficulties in maintaining stable flow over the entire acquisition period with adenosine infusion, the remaining eight dogs received a continuous infusion of 0.05 to 0.14 mg/kg/min of dipyridamole intravenously. Experiments where blood flow was not stable over the acquisition period or the collection of data was incomplete were excluded from further analysis. From a total of 22 experiments, 16 could be included for  $^{13}\text{N}$ -ammonia studies and 15  $^{15}\text{O}$ -water studies were analyzed. In these studies, mean variation of hyperemic blood flows based on doppler flow probe measurements was found to be  $4.9\% \pm 3.1\%$  during the initial 10 min.

### Tissue Assay

Following the last tracer study, the dogs were killed with a dose three times the initial dose of intravenous pentobarbital (90 mg/kg). Three 10-cm long needles were advanced through the chest at the image plane to define the orientation of the heart in the tomographic images. The heart was then excised, the right ventricle and atria discarded, and the left ventricle weighed. A 1-cm thick cross-sectional slice was cut along the needle insertion sites in the left ventricle. This roughly corresponded to the middle plane of the scanner. One centimeter slices were obtained on either side of the midplane yielding three slices per heart. Each of these three slices was then sectioned into samples weighing approximately 1 g. Each sample was weighed, transferred into counting vials, and the activity determined in a well counter. Whole myocardial blood flow averaged over these three slices was compared with blood flow derived from one midventricular plane obtained from the central tissue ring.

### Assessment of Flow by Microspheres

Myocardial blood flow was determined using the standard reference microspheres technique (11). Carbonized polystyrene microspheres [Dupont-NEN, size  $15 \pm 0.5 \mu\text{m}$  in diameter] were agitated by ultrasonification and resuspended with a vortex shaker. Approximately  $2 \times 10^6$  microspheres were injected with each acquisition. The microspheres were labeled with either  $^{46}\text{Sc}$  (980 keV, preset energy window 840–1048 keV),  $^{95}\text{Nb}$  (765 keV, 710–820 keV),  $^{113}\text{Sn}$  (393 keV, 360–440 keV) or  $^{141}\text{Ce}$  (150 keV, 127–175 keV). Both tissue and blood sample activity were measured using a sodium iodide well counter (model 5780 Packard). Compton cross-contamination between well counter channels were corrected using the “stripping” technique described by Heymann et al. (11). The blood and tissue activity counts were normalized to each other according to their weights.

### PET Data Analysis

**Definition of Regions of Interest.** The mid-ventricular image from the last frame of the  $^{13}\text{N}$ -ammonia acquisition was used to manually draw a region of interest (ROI) around the myocardium. After pharmacological intervention, the region was redefined to match the changing geometry of the cardiac chamber. The size of a typical region was between 10–15  $\text{cm}^2$ , the count

rate in the central plane was not higher than 95 kcts/sec immediately after tracer injection and was above 25 kcts/sec after 10 min. The regions positioned based on the  $^{13}\text{N}$ -ammonia image were also used to define the myocardium for the  $^{15}\text{O}$ -water studies at corresponding flow states, since myocardial definition was not possible on  $^{15}\text{O}$ -water images. A large myocardial region was taken for data analysis, covering the lateral, inferior and anterior wall of the myocardium. Partial volume and spillover effects were incorporated into the operational equation through the addition of a total blood volume parameter (TBV) (12). The result of that study revealed that this correction approach is independent of the size of the region, as long as the regions contain contributions from only myocardial tissue and blood pool. The ROIs were defined near the endocardial edge where they fulfilled the above stated conditions. They were stored and copied on both  $^{13}\text{N}$ -ammonia and  $^{15}\text{O}$ -water dynamic image sequences. Decay-corrected time-activity curves were then constructed for the myocardium in each study.

**Definition of the Blood Input Function.** Given the smaller heart in dogs (15–20 kg animals) and the relatively low spatial resolution of the PET camera (FWHM of 12.5 mm), we were not able to derive blood time-activity curves free from activity spillover from myocardium. As resolution distortions of the input function are not corrected in the model conception, we used the well counter-determined blood input function in the modeling procedure. Furthermore, this study was strictly designed to validate the accuracy of the proposed three-compartmental approach, in which case the best available input function should be taken.

However, it has been previously shown by several investigators (13–15) that in dynamic  $^{13}\text{N}$ -ammonia studies and with spatial resolutions provided by state-of-the-art PET cameras, curve data from left ventricular regions of interest can be used accurately as  $^{13}\text{N}$ -ammonia input functions. The results of these studies indicate that the usage of a well counter-determined input function in the presented study does not limit the general practicability of this method in a clinical setting.

**Tracer Model for  $^{13}\text{N}$ -Ammonia.** The kinetic properties of  $^{13}\text{N}$ -ammonia in myocardial tissue can be described in terms of a three-compartment model (Fig. 2). The first compartment, ( $C_a$ ), represents arterial blood in vascular space. The second compartment, ( $C_E$ ), represents extravascular space and is a conceptual construct of interstitial and intracellular tissue space. The third compartment, ( $C_G$ ), characterizes the accumulation of the metabolic product of  $^{13}\text{N}$ -ammonia within the cell. The sum of  $C_E$  and  $C_G$  equals  $C_T$ , the total tissue activity predicted by the model. The parameters  $k_2$  and  $k_3$  are true rate constants and have the dimension of [ $\text{min}^{-1}$ ]. The parameter  $K_1$  expresses the combined processes of radionuclide delivery by blood flow to the tissue and transmembranous extraction into the extravascular space of the tissue [ $\text{ml blood/g tissue/min}$ ].

The measured activity in a single positron emission tomographic image represents the averaged activity integral from the beginning ( $t_1$ ) to the end ( $t_2$ ) of the current data acquisition frame within a certain volume element. In addition, due to the finite spatial resolution of the PET, partial volume and cross-contamination of activity between blood and myocardium have to be considered in the model equation. Because the myocardial tissue wall is thinner than the spatial resolution of the tomograph, and the heart moves through the cardiac cycle, myocardial activity cannot be completely separated from blood pool activity of right and left ventricular chambers. Thus, the measured concentration

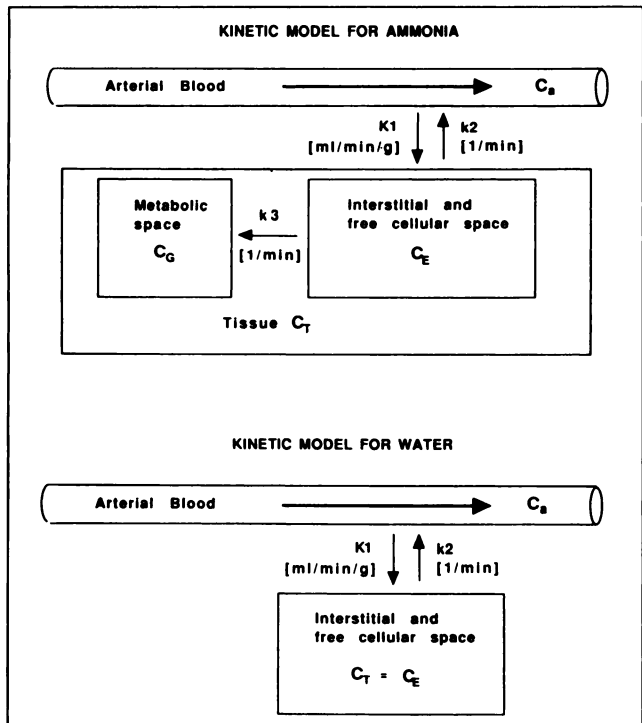


**FIGURE 2.** Three-compartment tracer kinetic model describing extraction and retention of  $^{13}\text{N}$ -ammonia in myocardial tissue (top).  $K_1$  and  $k_2$  are rate constants reflecting the exchange of  $^{13}\text{N}$ -ammonia between arterial blood ( $C_a$ ) and the interstitial and free cellular space ( $C_E$ );  $k_3$  represents metabolic trapping of  $^{13}\text{N}$ -ammonia in the metabolic space ( $C_G$ ). The kinetics of  $^{15}\text{O}$ -water are characterized by a two-compartment model (bottom). The rate constants  $K_1$  and  $k_2$  describe the exchange of  $^{15}\text{O}$ -water between vascular ( $C_a$ ) and extravascular space ( $C_T$ ).

by the PET scanner  $C_m$  can be expressed as:

$$C_m(t) = \frac{1}{(t_2 - t_1)} \cdot \left[ (1 - \text{TBV}) \rho_{\text{tissue}} \int_{t_1}^{t_2} C_T(t) dt + \text{TBV} \int_{t_1}^{t_2} C_a(t) dt \right] \quad \text{Eq. 1}$$

It is important to note that the model equations have been derived assuming that only myocardial tissue and blood occupy the volume of space represented by the ROI. Therefore, factors such as partial volume effect and cross-contamination of signal between blood and tissue are accounted for by the term  $(1 - \text{TBV})$  which represents the fraction of the volume occupied by tissue and  $\text{TBV}$  which is the fraction of the volume containing blood (8).

When blood activity determined by arterial sampling is used as the input function, it is necessary to correct for the time difference between the tracer's arrival in the myocardial tissue and its arrival at the arterial sampling site. Based on simulation studies, several investigators have reported errors as large as 10%–20% of the calculated flows by neglecting a Shift parameter (16). The Shift parameter was fitted as a fifth parameter in addition to the parameters  $K_1$ ,  $k_2$ ,  $k_3$  and  $\text{TBV}$ . Obviously, this parameter is not needed when the arterial input function is derived from a left ventricular region of interest as can be done for the larger sized human heart (14).

The prediction of tissue activity concentration  $C_m(t)$  by the

model was formulated in the following operational equation:

$$C_m(t) = \frac{1}{(t_2 - t_1)} \cdot \int_{t_1}^{t_2} \left\{ (1 - \text{TBV}) \rho_{\text{tissue}} \left[ \frac{K_1 k_3}{k_2 + k_3} \int_0^T C_a(u - \text{Shift}) du + \frac{K_1 k_2}{k_2 + k_3} \int_0^T C_a(u - \text{Shift}) \cdot \exp^{-(k_2 + k_3)(T - u)} du \right] + \text{TBV} \cdot C_a(T - \text{Shift}) \right\} dT. \quad \text{Eq. 2}$$

All data points acquired with the appropriate dynamic protocol (19 data points in case of the 10 min studies and 23 data points in case of the 30 min studies) were included into the model fit. All parameters  $K_1$ – $k_3$ ,  $\text{TBV}$  and Shift were simultaneously estimated using a nonlinear least-square fit of Equation 2 to the data. A value of 1.042 (g tissue/ml tissue) was used for the tissue density  $\rho_{\text{tissue}}$ .

It was reported by Schelbert et al. (6), that the permeability surface product (PS) of  $^{13}\text{N}$ -ammonia for the initial extraction fraction E is only slightly dependent on flow (PS [ml/100 g/min] = 108 + 2.34 F). When this experimental relation is used together with the Crone-Renkin (17,18) model for extraction,

$$E = [1 - \exp^{-\text{PS}/F}], \quad \text{Eq. 3}$$

the initial extraction fraction remains >90% for flows up to 600 ml/100 g/min. In our basic three-compartment model for  $^{13}\text{N}$ -ammonia, the unidirectional inflow rate constant  $K_1$  is directly proportional to flow assuming E to be 1.0. Myocardial blood flow ( $\text{MBF}_{\text{NH}_3}$ ) can be expressed as

$$\text{MBF}_{\text{NH}_3} [\text{ml/g/min}] = K_1 [\text{ml/g/min}]. \quad \text{Eq. 4}$$

*Correction of Arterial Input Function For Metabolites.* Nitrogen-13-ammonia and  $^{13}\text{N}$  metabolites in blood were determined as described previously (19) at 1, 3, 5 and 10 min after the  $^{13}\text{N}$ -ammonia injection and expressed as percent of total blood activity. The blood data was fitted to a function  $y = A t^{-B}$  to obtain best fit values for the parameters A and B. The measured arterial input function was then multiplied with the fitted exponential function to obtain the true  $^{13}\text{N}$ -ammonia concentration used in the model equation. Because spillover is affected by total  $^{13}\text{N}$  activity in blood, the non-metabolites corrected blood input function was always used for the spillover component. In order to determine the significance of metabolites correction for the flow estimates, results with and without correction were compared.

*Blood Flow Calculation Using  $^{15}\text{O}$ -Water.* Oxygen-15-water flow measurements were obtained by the established (20,21) two-compartment model using the principle of inert gas exchange developed by Kety (22,23) (Fig. 2). Oxygen-15 tissue activity is described by the following model equation:

$$C_m(t) = \frac{1}{(t_2 - t_1)} \cdot \int_{t_1}^{t_2} \left\{ (1 - \text{TBV}) \rho_{\text{tissue}} \cdot K_1 \int_0^T C_a(u - \text{Shift}) \cdot \exp^{-(k_2)(T - u)} du + \text{TBV} \cdot C_a(T - \text{Shift}) \right\} dT. \quad \text{Eq. 5}$$

The model equation was fitted to all obtained data points by nonlinear least-square regression yielding estimates for parameters  $K_1$ ,  $k_2$ ,  $\text{TBV}$  and Shift. Estimates of myocardial blood flow by  $^{15}\text{O}$ -water are based upon  $k_2$  estimates and the partition

coefficient of water for myocardial tissue. Since E of water into myocardial tissue is 1.0 (4,5), myocardial blood flow can be evaluated as:

$$MBF_{H_2O} [ml/g/min] = k_2 [l/min] \times p [ml/g], \quad \text{Eq. 6}$$

where p is the partition coefficient for water representing the equilibrium ratio of water content in the myocardium to that in blood. Throughout the study, we used a constant value of  $p = 0.96$ . This value has been determined from in vitro water content studies for blood and myocardial tissue (24).

**PET Microsphere Correlations.** The correlation of the PET derived flow data with microsphere determined blood flows was described using a linear least-square regression. A linear function  $y = kx + b$  was fitted to the data with the PET estimates representing the dependent variable and the microsphere estimates representing the independent variable. This analysis determined the correlation between the two independent techniques.

**Statistical Analysis.** To determine numerical values for fitted parameters, the model prediction was fitted to the discrete data points with a Marquardt-Levenberg algorithm. All fits were constrained to positive values for the parameters. For determination of parameter correlation, the correlation matrix was computed based on the model sensitivity matrix. A chi-square test was used to determine if the regression lines for  $^{13}\text{N}$ -ammonia and  $^{15}\text{O}$ -water differed significantly.

Baseline values for blood pressure, heart rate and relative blood flow were compared to pharmacologically vasodilated values using Student's paired t-test. Differences with a p value  $<0.05$  were considered statistically significant. The results are expressed as mean  $\pm$  standard deviation (SD).

## RESULTS

Eleven dogs were studied with tracer injection at baseline and following pharmacologic intervention. In these animals, 16  $^{13}\text{N}$ -ammonia studies and 15  $^{15}\text{O}$ -water studies could be performed under stable hemodynamic conditions. At baseline, systolic and diastolic blood pressure averaged  $119(\pm 8)/94(\pm 9)$  mm Hg and heart rate 140

( $\pm 14$ ) bpm, respectively. After dipyridamole or adenosine infusion, the systolic and diastolic blood pressure values decreased to  $103(\pm 14)/69(\pm 9)$  mm Hg and heart rate to  $125(\pm 28)$  bpm. Myocardial blood flow determined by microspheres ranged from 53 to 620 ml/100 g/min in the  $^{13}\text{N}$ -ammonia studies and 63 to 570 ml/100 g/min in the  $^{15}\text{O}$ -water studies.

### Nitrogen-13-Ammonia PET Studies

Typical time-activity curves obtained following injection of  $^{13}\text{N}$ -ammonia at two different flow conditions in the same dog are displayed in Figure 3. Nitrogen-13 concentration in the blood pool reached a maximum within 30 sec after tracer administration and rapidly declined during the first 2 min, after which it remained relatively constant without approaching zero. The tissue curves plateaued within 2 min after injection and did not change during the remainder of the study. The contrast between tissue and blood pool was high at baseline and increased significantly with increasing blood flows. Ten minutes postinjection, the mean myocardium to blood pool activity ratio was 4:1 at baseline flows and increased to 10:1 in the high flow states.

### Nitrogen-13-Metabolites in Blood

Nitrogen-13-ammonia is rapidly metabolized into amino acids and urea (19). Figure 4 shows the relative contribution of  $^{13}\text{N}$ -ammonia to  $^{13}\text{N}$  activity in canine blood for all 11 dogs studied within a flow range of 53–580 ml/100 g/min. Data were fitted to the function  $y = At^{-B}$ , where A and B represent parameter determined by nonlinear regression. Average values for A and B were not significantly different between baseline and high flow states, therefore all values were pooled together. The average  $^{13}\text{N}$ -ammonia content in blood as a function of time was determined as  $A = 90.20(\pm 6.15)$  and  $B = 0.661(\pm 0.179)$ .

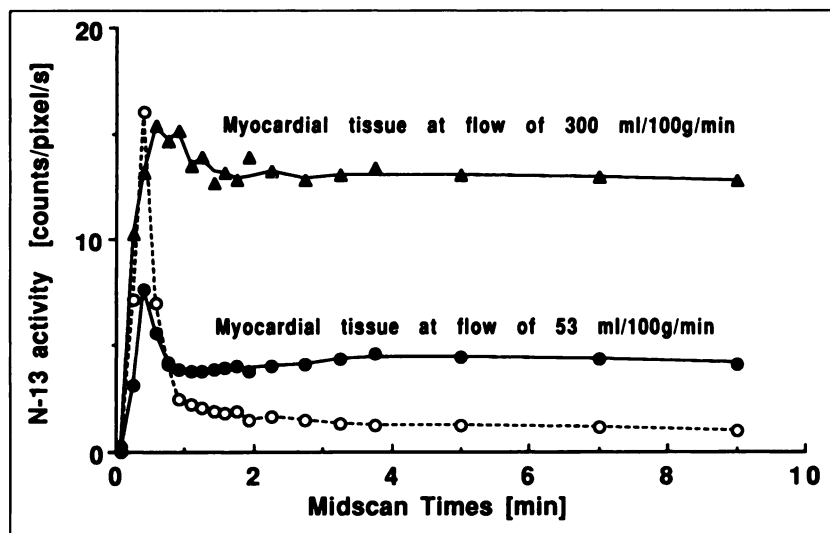


**FIGURE 3.** Baseline time-activity curves obtained from well counter blood (open circles) and a large myocardial region (closed circles). The myocardial tissue time-activity curve obtained at high flow (closed triangles) was scaled to the baseline input function. The nonlinear least squares fit (line) is shown for both tissue curves.

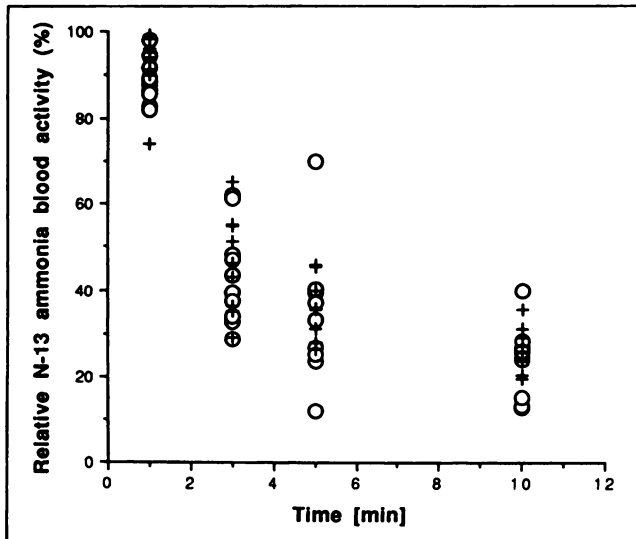


**FIGURE 4.** The relative  $^{13}\text{N}$ -ammonia blood activity expressed as the percentage of overall  $^{13}\text{N}$  activity present in the blood pool. Open circles represent the fate of  $^{13}\text{N}$ -ammonia at baseline flow states, (+) represents  $^{13}\text{N}$ -ammonia at pharmacologically vasodilated flow states. At all timepoints, mean values for both states were not significantly different.

#### Influence of Metabolites Correction on Model Parameters

The  $^{13}\text{N}$ -ammonia data were also analyzed without correcting for metabolites to examine the possibility of simplifying study protocols as well as to confirm our previous observations (8). Blood flow estimates determined with metabolites correction (MC) and without correction (NC) are plotted as a function of microsphere flows in Figures 5 and 6. The influence of metabolites correction appears to be negligible on the  $K_1$  (or blood flow) estimates.

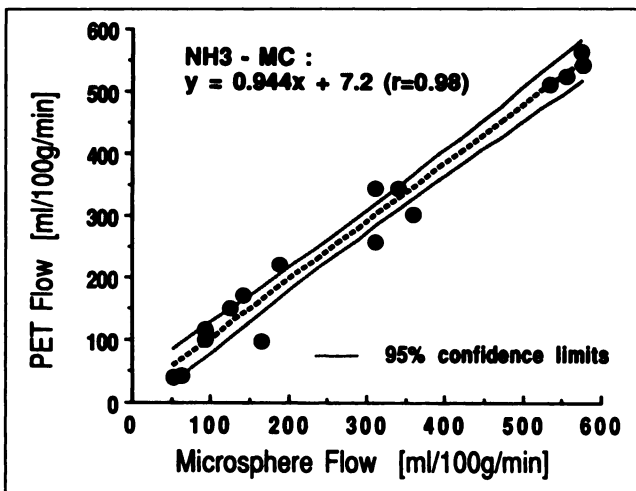


**FIGURE 5.** Myocardial blood flow estimates obtained with the  $^{13}\text{N}$ -ammonia technique using metabolites correction (MC) of the input function. Flow estimates are displayed as a function of microsphere determined flows. The broken line represents a least-square linear regression through the data together with the 95% confidence limits. Values for the slope, intercept and Pearson's  $r$  are given in the upper left corner.

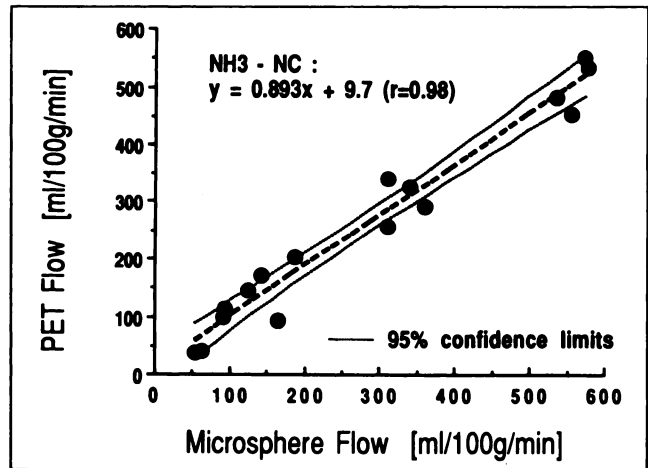


**FIGURE 6.** Myocardial blood flow estimates obtained with the  $^{13}\text{N}$ -ammonia technique using the noncorrected (NC) input function. Flow estimates are displayed as a function of microsphere determined flows. The broken line represents a least-square linear regression through the data together with the 95% confidence limits. Values for the slope, intercept and Pearson's  $r$  are given in the upper left corner.

Comparison between slope and intercept values before and after metabolites correction showed no statistically significant difference. However, there are significant changes in the value of  $k_3$  when the metabolites correction is not performed ( $p < 0.05$ ). The average value for  $k_3$  decreased from a value of  $0.332 \pm 0.206$  to  $0.061 \pm 0.048$  when metabolites correction was not applied to the blood input function. After metabolites correction, the rate constant for backdiffusion,  $k_2$ , slightly increased from a value of  $0.440 \pm 0.274$  to  $0.535 \pm 0.473$ .

#### Comparison of $^{13}\text{N}$ -Ammonia and $^{15}\text{O}$ -Water Derived Blood Flows

Myocardial blood flow was also determined with the  $^{15}\text{O}$ -water technique using a two-compartment model as described earlier. Blood flow estimates were determined for the same regions of interest as were used for the  $^{13}\text{N}$ -ammonia blood flow determination. Figure 7 shows the correlation between myocardial blood flow determined using  $^{15}\text{O}$ -water and myocardial blood flow obtained using radiolabeled microspheres. Both the  $^{13}\text{N}$ -ammonia as well as the  $^{15}\text{O}$ -water method showed an excellent correlation over a wide flow range with a slope close to unity as can be seen in Figures 5, 6 and 7.

To determine the statistical significance of the difference between the  $^{15}\text{O}$ -water and the  $^{13}\text{N}$ -ammonia methods, the slope and intercept parameters of the regression lines displayed in Figures 5, 6 and 7 were tested against each other using a chi-square test. All these differences were determined as statistically not significant.

#### DISCUSSION

The presented data indicate that myocardial blood flow can be quantified noninvasively by PET using  $^{13}\text{N}$ -am-

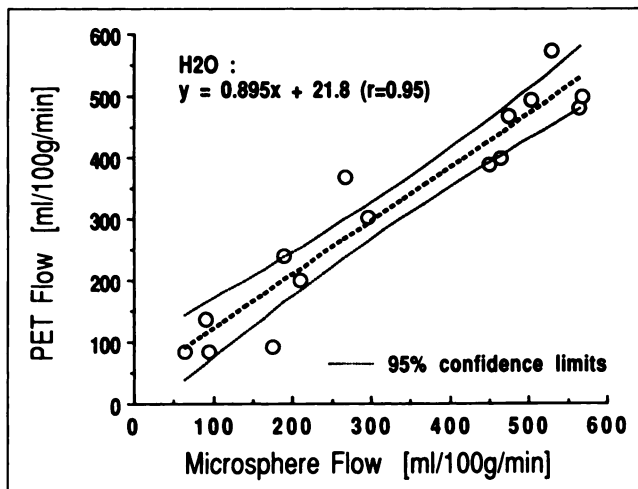


**FIGURE 7.** Myocardial blood flow values as predicted by the  $^{15}\text{O}$ -water method in comparison to radiolabeled microspheres. The broken line represents a least squares linear regression through the data together with the 95% confidence limits. Values for the slope, intercept and Pearson's  $r$  are given in the upper left corner.

monia and a three-compartment tracer kinetic model. Positron emission tomographic flow estimates were correlated linearly with measurements obtained by radiolabeled microspheres. Furthermore, flow estimates obtained with  $^{13}\text{N}$ -ammonia or  $^{15}\text{O}$ -water by PET agreed closely over the entire flow range studied. Thus,  $^{13}\text{N}$ -ammonia allows accurate assessment of myocardial blood flow which may be useful for the functional assessment of severity of coronary artery stenosis in patients with coronary artery disease.

### Myocardial Blood Flow Tracer

Oxygen-15-water represents an almost ideal PET blood flow tracer because it diffuses freely across cell membranes and is metabolically inert. Even at high flow states, tissue extraction of  $^{15}\text{O}$ -water is not diffusion limited and hence, tissue tracer retention correlates linearly with changes in myocardial blood flow (4). These physiologic advantages have made  $^{15}\text{O}$ -water the tracer of choice for cerebral blood flow studies. Since  $^{15}\text{O}$ -water is diffusible, tracer activity in blood and tissue rapidly equilibrate and are difficult to separate by scintigraphic means. In contrast to the brain, the heart is characterized by a larger tissue vascular space (8% to 11% heart versus 3% to 5% brain) (25,26). Furthermore, myocardial walls are relatively thin and are directly adjacent to the ventricular chambers. Therefore, the application of the  $^{15}\text{O}$ -water method in the heart requires subtraction of blood-pool activity for the identification of myocardial  $^{15}\text{O}$ -water tissue distribution. Such corrections are possible and provide accurate quantification of myocardial blood flow over a wide flow range as demonstrated in this and in many previous studies. However, the requirement of a separate blood-pool scan limits

the clinical application of diffusible blood flow tracers for the assessment of myocardial blood flow.

Several alternative blood flow tracers which are trapped in myocardium proportionately to blood flow have been introduced for PET imaging. Rubidium-82 and  $^{13}\text{N}$ -ammonia have been shown to provide high diagnostic accuracy for the qualitative detection of regional perfusion abnormalities in patients with coronary artery disease. The use of the retention of these tracers for the quantification of myocardial blood flow is limited by the nonlinear relationship between tracer retention and myocardial blood flow (7,27).

The tissue retention of  $^{13}\text{N}$ -ammonia is determined by the incorporation of the label into the amino acid pool in the form of glutamine. This metabolic step represents the rate limiting process of  $^{13}\text{N}$ -ammonia tissue retention. However,  $^{13}\text{N}$ -ammonia crosses tissue membranes as ammonium  $\text{NH}_4$  via passive diffusion and defines the initial extraction of the tracer from the vascular space. As previously shown, this first-pass extraction fraction changes very little with increasing blood flow. After the initial extraction of  $^{13}\text{N}$ -ammonia, the metabolic incorporation of the tracer competes with backdiffusion into the vascular space.

Based on these physiologic properties of  $^{13}\text{N}$ -ammonia, we have developed a three-compartment model which was designed to separate initial extraction from metabolic retention of the tracer. Assuming almost complete extraction of the tracer during first pass by myocardial tissue, the transport rate constant  $K_1$  directly reflects myocardial blood flow. Comparison of  $K_1$  estimates with myocardial blood flow in this study supports the validity of this assumption. In contrast to the rate constant  $k_3$ , which represents the metabolic retention of  $^{13}\text{N}$ -ammonia,  $K_1$  reflects the delivery of the tracer to the tissue. Quantitative imaging approaches which rely on the definition of tissue retention, require correction factors for the decreasing retention fraction at high flow states (7). These corrections are noise sensitive at high flows because tissue tracer concentrations change very little with increasing blood flow. In addition, these corrections rely upon a fixed relationship between MBF and ammonia metabolism (14).

### Partial Volume Effect

The accurate assessment of tracer extraction by myocardial tissue depends on the accuracy of the determination of tissue tracer concentration. Measurement of tissue tracer concentration is affected by the geometry of tissue under study. The thickness of the left ventricular wall is less than the spatial resolution of the PET instrumentation, which results in an underestimation of true tracer tissue concentration (partial volume effect) and significant cross-contamination of activity between myocardium and surrounding tissue (28). Previous approaches to correct for this possible error included the assumption of a constant

left ventricular wall thickness or the measurement of myocardial wall thickness by independent methods such as echocardiography (29). Based on the assumed or measured wall thickness, the tracer tissue concentration derived from images can be corrected for partial volume effects. Since the wall thickness of the left ventricle is not constant and increases during the cardiac cycle, depending on the contractile function, the use of an assumed myocardial wall thickness leads only to an approximation of ventricular tracer tissue concentration. The tracer kinetic model used in this study incorporates a correction term for the resolution distortions (12). Both effects are different representations of the finite resolution of the PET scanner. Formulating our model equation with one correction parameter TBV, we attempted to fit for both effects simultaneously, reducing the number of parameters in the fitting routine. Because each measured midscan activity concentration represents the average of many cardiac cycles, the acquired data provides only information about average partial volume and spillover contributions. (Geometrical correction approaches (25) assume a fixed wall thickness, a restriction never fulfilled in reality.) By incorporating the resolution effects in the model, the dynamic behavior of the radionuclide concentration in blood and tissue enable the isolation of the true myocardial tissue concentration. The data in this study demonstrate that this approach resulted in good agreement between absolute flow obtained through PET and microsphere flow determination in the normal canine myocardium. This method clearly simplifies the positron emission tomographic blood flow measurement without the need of wall thickness measurements by independent methods. Further studies are required for validation of this approach in areas of thin walls.

## CONCLUSION

The use of a three-compartment model for  $^{13}\text{N}$ -ammonia allows the quantification of myocardial blood flow over a wide range. Correction for  $^{13}\text{N}$ -labeled metabolites in blood is not necessary, simplifying the clinical application of this approach. In contrast to  $^{15}\text{O}$ -water,  $^{13}\text{N}$ -ammonia benefits from superior imaging quality allowing accurate definition of regions of interest without an additional blood-pool scan. Thus, the  $^{13}\text{N}$ -ammonia method allows the quantitative evaluation of regional myocardial blood flow using a simple acquisition protocol, which may be useful in the characterization of patients with coronary artery disease.

## ACKNOWLEDGMENTS

The authors thank Steve Toorongian, MS, William Walker, MS and Alaa El-Deen Mourad, PhD of the Cyclotron Unit for preparation of tracer and John Caraher, MS, for technical assistance during the PET studies. They also appreciate Tina Bennett's skillful secretarial assistance in preparing the manuscript. This work was carried out during the tenure of an established investi-

gatorship of Dr. Markus Schwaiger from the American Heart Association and was supported in part by the National Institutes of Health, Bethesda, MD (RO1 HL41047-01) and the Department of Energy, Washington, DC (DOE 89-035). Dr. Otto Muzik was supported by the Austrian Erwin Schroedinger Foundation project # J0473-MED. Dr. Rob Beanlands is a research fellow supported by the Heart and Stroke Foundation of Canada.

## REFERENCES

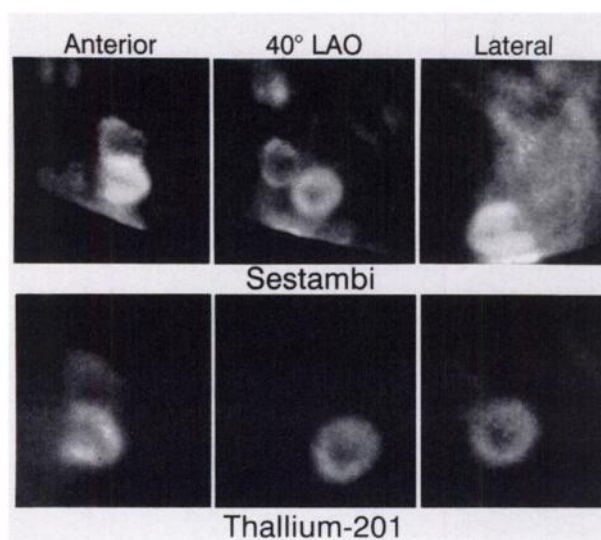
- Gould KL, Kirkeeide RL, Buchi M. Coronary flow reserve as a physiologic measure of stenosis severity. *J Am Coll Cardiol* 1990;15:459-474.
- Demer LL, Gould KL, Kirkeeide R. Assessing stenosis severity: coronary flow reserve, collateral function, quantitative coronary angiography, positron imaging, and digital subtraction angiography. A review and analysis. *Prog Cardiovasc Dis* 1988;30:307-22.
- White C, Wilson R, Marcus M. Methods of measuring myocardial blood flow in humans. *Prog Cardiovasc Dis* 1988;31:79-94.
- Bergmann SR, Herrero P, Markham J, Weinheimer CJ, Walsh MN. Noninvasive quantification of myocardial blood flow in human subjects with  $^{15}\text{O}$ -water and positron emission tomography. *J Am Coll Cardiol* 1989;14:639-652.
- Iida H, Kanno I, Takahashi A, et al. Measurement of absolute myocardial blood flow with  $^{15}\text{O}$ -water and dynamic positron emission tomography. Strategy for quantification in relation to the partial volume effect. *Circulation* 1988;78:104-115.
- Schelbert H, Phelps M, Huang S, et al. N-13-ammonia as an indicator of myocardial blood flow. *Circulation* 1981;63:1259-1272.
- Shah A, Schelbert HR, Schwaiger M, et al. Measurement of regional myocardial blood flow with  $^{13}\text{N}$ -ammonia and PET in intact dogs. *J Am Coll Cardiol* 1985;5:92-100.
- Hutchins GD, Schwaiger M, Rosenspire KC, Krivokapich J, Schelbert H, Kuhl DE. Non-invasive quantification of regional myocardial blood flow in the human heart using  $^{13}\text{N}$ -ammonia and dynamic positron emission tomographic imaging. *J Am Coll Cardiol* 1990;15:1032-1042.
- Position of the American Heart Association on research animal use. *Circulation* 1985;71:849A-50A.
- Kearfott K, Carroll L. Evaluation of the performance characteristics of the PC 4600 positron emission tomograph. *J Comput Assist Tomogr* 1984;8:502-513.
- Heymann MA, Payne BD, Hoffman JE, Rudolph AM. Blood flow measurements with radionuclide labeled particles. *Prog Cardiovasc Dis* 1977;20:55-79.
- Hutchins G, Caraher J, Raylman R. A region of interest strategy for minimizing resolution distortions in quantitative myocardial PET studies. *J Nucl Med* 1992;33:1243-1250.
- Weinberg IN, Huang SC, Hoffman EJ, et al. Validation of PET-acquired input functions for cardiac studies. *J Nucl Med* 1988;29:241-247.
- Krivokapich J, Smith GT, Huang SC, et al.  $^{13}\text{N}$ -ammonia myocardial imaging at rest and with exercise in normal volunteers. Quantification of absolute myocardial perfusion with dynamic positron emission tomography. *Circulation* 1989;80:1328-1337.
- Bellina C, Parodi O, Camici P, et al. Simultaneous in vitro and in vivo validation of N-13-ammonia for the assessment of regional myocardial blood flow. *J Nucl Med* 1990;31:1335-1343.
- Meyer E. Simultaneous correction for tracer arrival delay and dispersion in CBF measurements by the  $^{15}\text{O}$ -water autoradiographic method and dynamic positron emission tomography. *J Nucl Med* 1989;30:1069-1078.
- Crone C. Permeability of capillaries in various organs as determined by use of the indicator diffusion method. *Acta Physiol Scand* 1963;58:292.
- Renkin E. Transport of potassium-42 from blood tissue in isolated mammalian skeletal muscles. *Am J Physiol* 1959;197:1205.
- Rosenspire KC, Schwaiger M, Mangner TJ, Hutchins GD, Sutorik A, Kuhl DE. Metabolic fate of  $^{13}\text{N}$ -ammonia in human and canine blood. *J Nucl Med* 1990;31:163-167.
- Herscovitch P, Raichle ME, Kilbourn MR, Welch MJ. Positron emission tomography measurement of cerebral blood flow and permeability-surface area product of water using  $^{15}\text{O}$ -water and  $^{11}\text{C}$ -butanol. *J Cereb Blood Flow Metab* 1987;7:527-542.
- Bergmann SR, Fox KA, Rand AL, et al. Quantification of regional myocardial blood flow in vivo with  $^{15}\text{O}$ -water. *Circulation* 1984;70:724-733.
- Kety SS. The theory and applications of the exchange of inert gas at the lung and tissues. *Pharmacol Rev* 1951;3:1-41.



23. Kety SS. Measurement of local blood flow by the exchange of an inert, diffusable substance. *Methods Med Res* 1960;8:228-236.
24. Lammertsma AA, Jones T, Frackowiak RS, Lenzi GL. A theoretical study of the steady-state model for measuring regional cerebral blood flow and oxygen utilization using  $^{15}\text{O}$ . *J Comput Assist Tomogr* 1981;5:544-550.
25. Henze E, Huang SC, Ratib O, Hoffman E, Phelps ME, Schelbert HR. Measurements of regional tissue and blood pool radiotracer concentrations from serial tomographic images of the heart. *J Nucl Med* 1983;24:987-996.
26. Koeppel R, Hutchins G, Rothley J, Hichwa R. Examination of assumptions for cerebral blood flow studies in PET. *J Nucl Med* 1986;26:536-545.
27. Mullani N, Goldstein R, Gould K, et al. Perfusion imaging with rubidium-82: I. Measurement of extraction and flow with external detectors. *J Nucl Med* 1983;24:898-906.
28. Hoffmann EJ, Huang SC, Phelps ME. Quantitation in positron emission computed tomography. I. Effect of object size. *J Comput Assist Tomogr* 1979;299-308.
29. Wisenberg G, Schelbert H, Hoffman E, et al. In vivo quantitation of regional myocardial blood flow by positron emission tomography. *Circulation* 1981;63:1248-58.

(continued from page 5A)

## FIRST IMPRESSIONS



### **PATIENT INFORMATION**

A 63-yr-old female with atypical chest pain was referred for exercise thallium imaging to rule out coronary artery disease. The patient had submaximal exercise into Stage 2, achieving 7 mets with no angina or ST changes. A few days later, adenosine  $^{99m}\text{Tc}$ -sestamibi imaging was done because the exercise test was submaximal. Both thallium and sestamibi images showed normal perfusion patterns in the heart, however, there was a large extracardiac area of intense uptake. The patient had a biopsy proven  $6 \times 7$  cm infiltrating ductal carcinoma of the left breast

### **TRACER**

$^{201}\text{Tl}$  3 mCi (111 MBq) and  $^{99m}\text{Tc}$ -sestamibi 20 mCi (740 MBq).

### **ROUTE OF ADMINISTRATION**

Intravenous injection.

### **IMAGING TIME AFTER INJECTION**

10 min for thallium and 60 min for sestamibi.

### **STRUMENTATION**

Siemens gama camera/computer system.

### **COMPUTER SET UP**

128  $\times$  128 word mode matrix, 8 minutes per view.

### **CONTRIBUTORS**

Jaetae Lee, Kyubo Lee, Jaekyeong Heo and Abdulmassih S. Iskandrian.

### **INSTITUTION**

Kyungpook National University Hospital, Taegu, South Korea and the Philadelphia Heart Institute, Presbyterian Medical Center, Philadelphia, PA.